Accurate Magnetic Shell Approximations with Magnetostatic Finite Element Formulations by a Subdomain Approach

Vuong Dang Quoc
Department of Electrical and Electronic Equipment
School of Electrical Engineering
Hanoi University of Science and Technology
Hanoi, Vietnam
vuong.dangquoc@hust.edu.vn

***Abstract*—This paper presents a subproblem approach with h-conformal magnetostatic finite element formulations for treating the errors of magnetic shell approximation, by replacing volume thin regions by surfaces with interface conditions. These approximations seem to neglect the curvature effects in the vicinity of corners and edges. The process from the surface-to-volume correction problem is presented as a sequence of several subdomains, which can be composed to the full domain, including inductors and thin magnetic regions. Each step of the process will be separately performed on its own subdomain and submesh instead of solving the problem in the full domain. This allows reducing the size of matrix and time computation.**

Keywords-magnetostatic finite element formulation; magnetic scalar potential; magnetic field; magnetic shell; subproblem approach

I. INTRODUCTION

The local fields in magnetic shells are approximated by a priori 1-D analytical distributions across the shell thicknesses [1, 2]. This means that the interior of volume thin regions is not meshed and is introduced by surfaces with impedance-type Interface Conditions (ICs) linked to the inner-analytical distributions. This leads to negligible edges and corners of magnetic shells, increasing with thickness. In order to overcome this disadvantage, the Sub-Problem Method (SPM) for the magnetodynamic problem with dual formulation has been proposed for one-way coupling [3-10]. In this development, a subdomain technique based on the SPM is extended for the $\boldsymbol{h}$- conformal magnetostatic finite element formulation in order to improve the local fields (magnetic scalar potential, magnetic flux density and magnetic field) appearing around the edges and corners of magnetic shells. The idea of the method is to perform subdomain solving in three steps (Figure 1):

- Step 1: A lower subdomain attending with stranded inductors is first considered on a simplified mesh without any magnetic shells.
- Step 2: A shell with the very coarse mesh that does not contain stranded inductors anymore is then added.
- Step 3: A volume correction replacing the magnetic shell Finite Element (FE) by an actual thin region is introduced to improve shell inaccuracies.

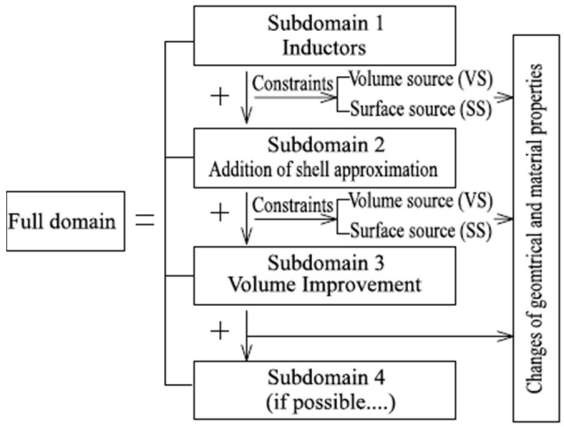

Fig. 1. Devision of a full domain into three steps.

The relation between steps is constrained by Volume Source (VS) expressed changes of the material propoerties or Surface Sources (SS) presented changes of ICs. In each step, the problem is independently solved in an individual sub-mesh and its surrounding without depending on other meshes, which allow to distinct mesh refinements. The method is applied on a practical problem.

II. MAGNETOSTATIC PROBLEMS

A canonical magnetostatic problem q presented at step q is solved in a domain Ω_q, with boundary $\partial\Omega_q = \Gamma_q = \Gamma_{h,q} \cup \Gamma_{e,q}$. Maxwell's equations, constitutive laws and boundary conditions (BCs) of the problem q give [3-11]:

$$\text{curl}\, \boldsymbol{h}_q = \boldsymbol{j}_q, \text{div}\boldsymbol{b}_q = 0 \quad \text{(1a-b)}$$

$$\boldsymbol{b}_q = \mu_q \boldsymbol{h}_q + \boldsymbol{b}_{s,q} \quad \text{(2)}$$

Corresponding author: Vuong Dang Quoc

$$\boldsymbol{n}\cdot\boldsymbol{b}_q|_{\Gamma_{e,q}}=0,\quad \left[\boldsymbol{n}\cdot\boldsymbol{b}_q\right]_{\gamma_q}=\boldsymbol{b}_{f,q} \quad \text{(3a-b)}$$

where $\boldsymbol{h}_q$ is the magnetic field (A/m), $\boldsymbol{b}_q$ is the magnetic flux density (T), $\boldsymbol{j}_q$ is the electric current density (A/m^2), μ_q is the magnetic permeability (H/m) and $\boldsymbol{n}$ is the unit normal exterior to Ω_q. The source field $\boldsymbol{b}_{s,q}$ in (2) is a VS that accounts for volume changes of permeability (μ_q) from the current problem to the next problem μ_p (q =p), i.e.:

$$\boldsymbol{b}_{s,p}=\left(\mu_p-\mu_q\right)\boldsymbol{h}_q. \quad (4)$$

The notation $[\cdot]_{\gamma_q}=|_{\gamma_q^+}-|_{\gamma_q^-}$ is the discontinuity of a quantity across the negative and positive sides of any interface γ_q in Ω_q. The field $\boldsymbol{b}_{f,q}$ is a SS between subdomains [3-10]. In addition, the magnetic field $\boldsymbol{h}_q$ in (1a) is split in two parts $\boldsymbol{h}_{s,q}$ and $\boldsymbol{h}_{r,q}$, i.e. $\boldsymbol{h}_q=\boldsymbol{h}_{s,q}+\boldsymbol{h}_{r,q}$, where $\boldsymbol{h}_{r,q}$ is the reaction field and $\boldsymbol{h}_{s,q}$ is a source magnetic field due to the imposed current density $\boldsymbol{j}_{s,q}$ ($\text{curl}\,\boldsymbol{h}_{s,q}=\boldsymbol{j}_{s,q}$).

III. SEQUENCE OF FE WEAK FORMULATIONS

A. Weak Formulation for Inductor Model - Step 1 (SP q)

The magnetostatic weak formulation ($\boldsymbol{h}_q-\Phi$) for Step 1 (SP q) is obtained via the magnetic Gauss's law (1b), i.e. [1, 2]:

$$\begin{gathered}-\left(\mu_q\boldsymbol{h}_{s,q},\text{grad}\Phi_q'\right)_{\Omega_q}+\left(\mu_q\text{grad}\Phi_q,\text{grad}\Phi_q'\right)_{\Omega_q}\\ +<\boldsymbol{n}\cdot\boldsymbol{b}_q,\Phi_q'>_{\Gamma_{e,q-\gamma_q}}+<-\left[\boldsymbol{n}\cdot\boldsymbol{b}_q\right]_{\gamma_q},\Phi_q'>_{\gamma_q}=0, \quad (5)\\ \forall\Phi_q'\in H_{h,q}^{10}\left(\Omega_q\right)\end{gathered}$$

where $H_{h,q}^{10}\left(\Omega_q\right)$ is a function space presented in Ω_q including the basis functions for Φ_q as well as for the test function Φ_q'. Notations of $(.,.)_{\Omega_q}$ and $\langle.,.\rangle_{\Gamma_q}$ are respectively the volume integral in Ω_q the surface integral on Γ_q, of the product of their vector field arguments. The surface term $<\boldsymbol{n}\cdot\boldsymbol{b}_q,\Phi_q'>_{\Gamma_{e,q-\gamma_q}}$ in (5) is considered as a natural BC of type (3a), usually zero.

B. Weak Formulation for Magetnic Shell Model - Step 2 (SP p)

The shell model (SP p) is defined via the last term in (5). The weak form of SP p, is [1, 2]:

$$\begin{gathered}\left(\mu_p\text{grad}\Phi_p,\text{grad}\Phi_p'\right)_{\Omega_p}+<\boldsymbol{n}\cdot\boldsymbol{b}_p,\Phi_p'>_{\Gamma_{e,p-\gamma_p}}\\ +<\left[\boldsymbol{n}\cdot\boldsymbol{b}_p\right]_{\gamma_p},\Phi_p'>_{\gamma_p}=0,\forall\Phi_p'\in H_{h,q}^{10}\left(\Omega_q\right) \quad (6)\end{gathered}$$

The trace discontinuity term $<\left[\boldsymbol{n}\cdot\boldsymbol{b}_p\right]_{\gamma_p},\Phi_p'>_{\gamma_p}$ in (6) is given as [4]:

$$\begin{gathered}<\left[\boldsymbol{n}\cdot\boldsymbol{b}_p\right]_{\gamma_p},\Phi_p'>_{\gamma_p}=\\ <\left[\boldsymbol{n}\cdot\boldsymbol{b}_p\right]_{\gamma_p},\Phi_{c,p}'>_{\gamma_p}+<\boldsymbol{n}\cdot\boldsymbol{b}_p|_{\gamma_p^+},\Phi_{d,p}'>_{\gamma_p^+} \quad (7)\end{gathered}$$

In addition, the term $<\left[\boldsymbol{n}\cdot\boldsymbol{b}_p\right]_{\gamma t,p},\Phi_{c,p}'>_{\gamma t,p}$ in (7) is obtained from [1, 2]:

$$\begin{gathered}<\left[\boldsymbol{n}\cdot\boldsymbol{b}_p\right]_{\gamma_p},\Phi_{c,p}'>_{\gamma_p}=-<\mu_p d_p\boldsymbol{h}_{s,p},\text{grad}\Phi_p'>_{\gamma_p}\\ +<\mu_p d_p\text{grad}\Phi_p,\text{grad}\Phi_p'>_{\gamma_p} \quad (8)\end{gathered}$$

The remaining term $<\boldsymbol{n}\cdot\boldsymbol{b}_p|_{\gamma_p^+},\Phi_{d,p}'>_{\gamma_p^+}$ in (7) is weakly presented via the surface source integral term, i.e.:

$$\begin{gathered}<\boldsymbol{n}\cdot\boldsymbol{b}_p|_{\gamma_p^+},\Phi_{d,p}'>_{\gamma_p^+}=-<\boldsymbol{n}\cdot\boldsymbol{b}_q|_{\gamma_p^+},\Phi_{d,p}'>_{\gamma_p^+}=\\ (\mu_q\text{grad}\Phi_q,\text{grad}\Phi_{d,p}')_{\Omega_p^+=\gamma_p^+}+(\mu_q\boldsymbol{h}_{s,q},\text{grad}\Phi_{d,p}')_{\Omega_p^+=\gamma_p^+}\\ =-\boldsymbol{b}_{f,q} \quad (9)\end{gathered}$$

The volume integrals in (9) are also limited to a single layer of FEs on the positive side of Ω_p^+ touching γ_p^+ [4-10]. By substituting (9) and (8) into (6), the weak form of SP p is rewritten as:

$$\begin{gathered}(\mu_p\text{grad}\Phi_p,\text{grad}\Phi_p')_{\Omega_p}-<\mu_p d_p\boldsymbol{h}_{s,p},\text{grad}\Phi_p'>_{\Gamma_{t,p}}+\\ \mu_p d_p\text{grad}\Phi_p,\text{grad}\Phi_p'>_{\Gamma_{t,p}}-(\mu_q\text{grad}\Phi_q,\text{grad}\Phi_{d,p}')_{\Omega_p^+}\\ +(\mu_q\boldsymbol{h}_{s,q},\text{grad}\Phi_{d,p}')_{\Omega_p^+}=0,\quad\forall\Phi_p'\in H_{h,p}^{10}\left(\Omega_p\right) \quad (10)\end{gathered}$$

At the discrete mesh, the source fields Φ_q and $\boldsymbol{h}_{s,q}$, initially in mesh of SP q, have to be transferred to the mesh of SP p via a projection method [15-17].

C. Weak Formulation for Volume Correction - Step 3 (SP k)

The weak form of SP k is finally established via a VS given by (2):

$$\begin{gathered}(\mu_k\text{grad}\Phi_k,\text{grad}\Phi_k')_{\Omega_k}-((\mu_k-\mu_p)\text{grad}\Phi_p,\text{grad}\Phi_k')_{\Omega_k}\\ +(\mu_k-\mu_p)((\boldsymbol{h}_{s,p}-\text{grad}\Phi_k'),\text{grad}\Phi_k')_{\Omega_k}+\\ <\boldsymbol{n}\cdot\boldsymbol{b}_k,\Phi_k'>_{\Gamma_{e,k-\gamma_k}}+<[\boldsymbol{n}\cdot\boldsymbol{b}_k]_{\gamma_k},\Phi_k'>_{\gamma_k}=0\\ \forall\Phi_k'\in H_{h,k}^{10}(\Omega_k) \quad (11)\end{gathered}$$

At the discrete mesh, the source quantities Φ_p and $\boldsymbol{h}_{s,p}$ in (11), defined in previous meshes (SP q and SP p) are also projected to the mesh of SP k via a projection method (see Section D). In addition, the discontinuity of SP p in SP k has to be removed by fixing as:

$$<[\boldsymbol{n}\cdot\boldsymbol{b}_k]_{\gamma_k},\Phi_k'>_{\gamma_k}=-<[\boldsymbol{n}\cdot\boldsymbol{b}_p]_{\gamma_k},\Phi_k'>_{\gamma_k} \quad (12)$$

D. Transformation of Solutions between Sub-meshes

As presented above, the source fields Φ_q and $\boldsymbol{h}_q$ obtained from the previous meshes of SPi (e.g. SP q) are transferred to the mesh of SP p, i.e. [15-17]:

$$(\boldsymbol{h}_{q,p-proj},\boldsymbol{h}')_{\Omega_{s,p}}=(\boldsymbol{h}_q,\boldsymbol{h}')_{\Omega_{s,p}},\quad\forall\boldsymbol{h}'\in H_{h,p}^{1}\left(\Omega_{s,p}\right) \quad (13)$$

where $\forall\boldsymbol{h}'\in H_{h,p}^{1}\left(\Omega_{s,p}\right)$ is a curl-conform function space for the p-projected source $\boldsymbol{h}_{q,p-proj}$ (the projection of $\boldsymbol{h}_{q,p-proj}$ on mesh of SP p) and the test function $\boldsymbol{h}'$ defined on $\Omega_{s,p}$.

In the same way, the magnetic scalar potential Φ_p, can project the grad of Φ_q in the mesh of SP q to the mesh of SP p, i.e. [9]:

$$\begin{gathered}(\text{grad}\Phi_{q,p-proj},\text{grad}\Phi')_{\Omega_{s,p}}=(\text{grad}\,\Phi_q,\text{grad}\Phi')_{\Omega_{s,p}}\\ \forall\Phi'\in H_{h,p}^{10}\left(\Omega_p\right) \quad (14)\end{gathered}$$

where $\Phi'\in H_{h,p}^{10}\left(\Omega_p\right)$ is the grad-conform function space for the p-projected source $\Phi_{q,p-proj}$ (the projection of Φ_q on mesh of SP p) and the test function Φ' defined on $\Omega_{s,p}$.

IV. APPLICATION TEST

The practical test is a shielded problem. It consists of a plate located in the middle of two stranded inductors carrying a magnetomovetive force of 1000 ampere-turns (Figure 2). The magnetic shields (screen up and down) cover the plate and the stranded inductors, for $\mu_{r,shield}$=1 and $\mu_{r,plate}$=200. The test is performed in the 2-D case. As a sequence, the test at hand is performed in three steps. The solutions on the magnetic scalar potential Φ of each subdomain are illustrated in Figure 3. An initial problem SP q including the stranded inductors alone is solved in a sub-domain without the shielding plate and screens up and down (Figure 3(a), Φ_q).

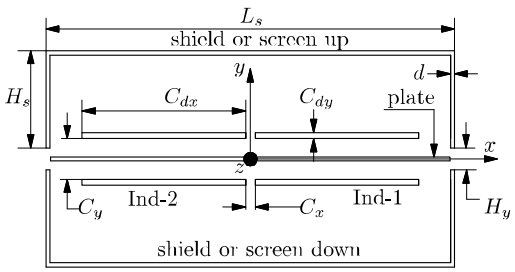

Fig. 2. Geometry of a 2-D shielding problem (d=3÷7.5mm, L_{pl}=2m, L_s=2m+2d, Hs=0.4m, H_y=0.14m, C_{dx}=0.8m, C_{dy}=0.01m, C_y=0.2m, C_x=0.05m).

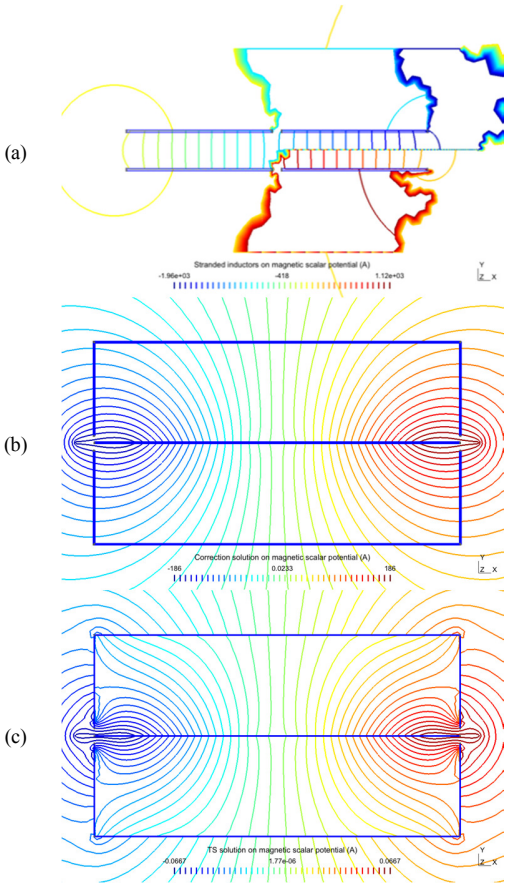

Fig. 3. Distribution of magnetic scalar potentials for (a) the stranded inductors alone SP q (Φ_q), (b) addition of TS solution SP p (Φ_p), and (c) volume correction SP k (Φ_k) for thickness d=5mm).

The shell approximation SP p that does not include the stranded inductors anymore is then added (Figure 3(b), Φ_p). The volume improvements covering the shielding plate and screen up and down are finally introduced to overcome the shell approximations [1, 2], for d=5mm, $\mu_{r,shield}$ =1 and $\mu_{r,plate}$ =200 (Figure 3(c), Φ_k). In a similar way, the distribution of magnetic flux density for each subdomain obtained in each step is shown in detail in Figure 4. The sequence from Step 1 (SP q) → Step 2 (SP p) → Step 3 (SP k) is pointed out from *top* to *bottom*, for thickness d=5mm.

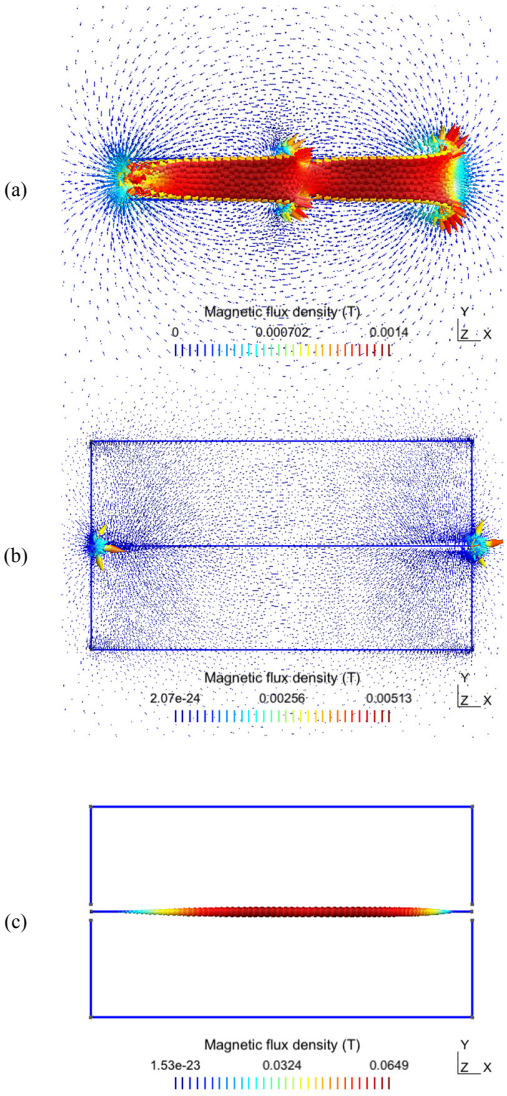

Fig. 4. Distribution of magnetic flux densities $\boldsymbol{b} = \mu(\boldsymbol{h}_s - \text{grad}\,\Phi)$ for (a) stranded inductors alone SP q, (b) addition of the shell model SP p, and (c) volume correction SP k for thickness d=5mm.

The significant errors on the magnetic flux densities of the shell approximation solution (SP p) along the plate are corrected by the volume correction (SP k) indicated in Figure 5. The error reaches approximately 35% near the middle of the plate, for d=5mm ($\mu_{r,shield}$=1 and $\mu_{r,late}$=200). The volume

solution is then checked to be similar to the reference solution in the computation from the traditional finite element method (FEM) [12-14].

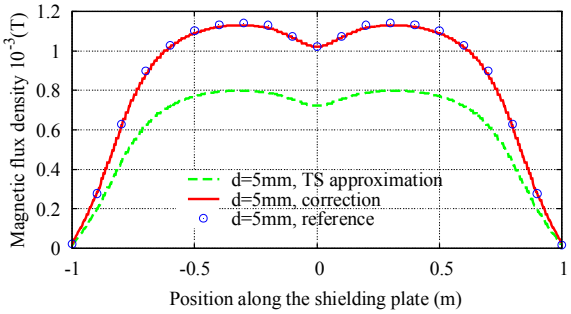

Fig. 5. Magnetic flux density on the shell solution, volume correction and reference solution along the plate, for d=5mm.

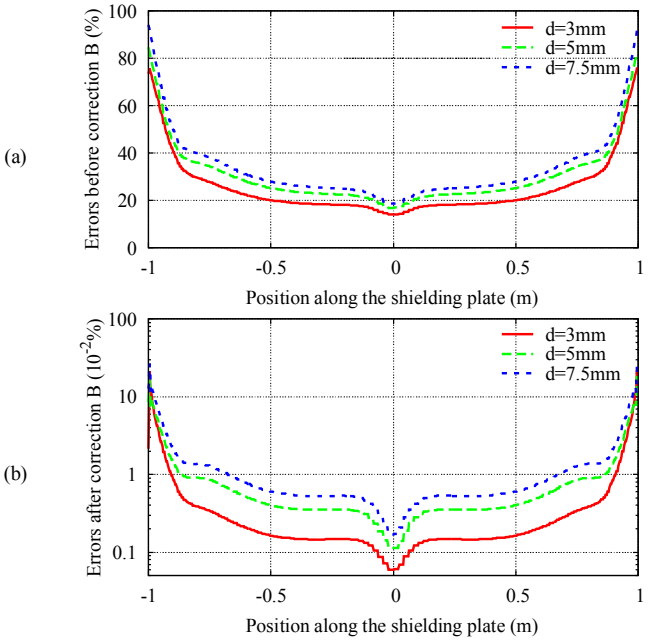

Fig. 6. TS inaccuracy on the magnetic flux density along the shielding plate (a) before making a correction and (b) after the correction for different values d.

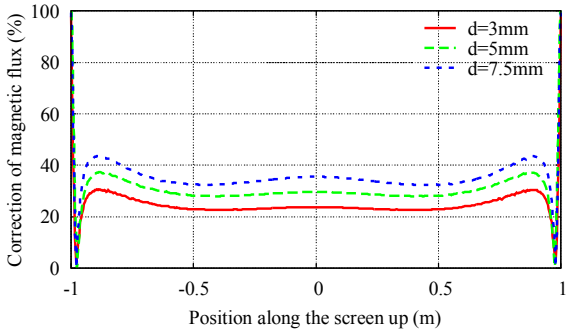

Fig. 7. Relative (improvement) correction of the magnetic flux density along the screen up for different values of d.

The relative inaccuracy on the magnetic flux densities before making corrections is presented in Figure 6 for various thicknesses. The error can reach 90% at the end regions of the plate, for d=7.5 mm, and 75% for smaller thickness d=3 mm for $\mu_{r,shield}$=1 and $\mu_{r,plate}$=200. Accurate local improvement with volume correction SP k after improving are less than 15% for d=7.5mm near the plate end, or 10% for d=3 mm. It is worth noting that the error is less than 1% in the middle of the plate for both cases. The relative improvement (correction) of the TS magnetic flux along the screen up is presented in Figure 7 for different screen thicknesses. It can reach a percentage up to 47% near the edge of the screen up, for d=7.5mm. It reduces to about 40% for d=5 mm, or 30% for d=3mm, with $\mu_{r,shield}$=1 and $\mu_{r,plate}$=200.

V. DISCUSSION AND CONCLUSION

In this research, a subdomain technique for coupling thin magnetic shells has been successfully developed with ***h***-conformal magnetostatic finite element formulations for improving the errors of the magnetic scalar potential, magnetic flux density, and magnetic flux around the edges and corners appearing from the magnetic shell approximation [1, 2]. The obtained results of the method were found to be quite similar to the reference solution in the computation of the traditional FEM [12-14]. The proposed technique has been successfully carried out with a three step sequence. In the future, it could be extended to the case of multilayer-TS with different characteristics.

The source-code of the method has been extended from the one subproblem method that was developed by the author with the help of Patrick Dular and Christophe Geuzaine at the Deparment of Electrical Engineering and Computer Science, University of Liege, Belgium. It will be ran in the background of the Getdp and Gmsh (http://getdp.info and http://gmsh.info) as open source code.

REFERENCES

[1] C. Geuzaine, P. Dular, and W. Legros, "Dual formulations for the modeling of thin conducting magnetic shells," *COMPEL - The International Journal for Computation and Mathematics in Electrical and Electronic Engineering*, vol. 18, no. 3, pp. 385–398, Jan. 1999, doi: 10.1108/03321649910274946.

[2] C. Geuzaine, P. Dular, and W. Legros, "Dual formulations for the modeling of thin electromagnetic shells using edge elements," *IEEE Transactions on Magnetics*, vol. 36, no. 4, pp. 799–803, Jul. 2000, doi: 10.1109/20.877566.

[3] P. Dular and R. V. Sabariego, "A Perturbation Method for Computing Field Distortions Due to Conductive Regions With $\mmb h$ -Conform Magnetodynamic Finite Element Formulations," *IEEE Transactions on Magnetics*, vol. 43, no. 4, pp. 1293–1296, Apr. 2007, doi: 10.1109/TMAG.2007.892401.

[4] P. Dular, R. V. Sabariego, C. Geuzaine, M. V. Ferreira da Luz, P. Kuo-Peng, and L. Krähenbühl, "Finite Element Magnetic Models via a Coupling of Subproblems of Lower Dimensions," *IEEE Transactions on Magnetics*, vol. 46, no. 8, pp. 2827–2830, Aug. 2010, doi: 10.1109/TMAG.2010.2044028.

[5] P. Dular, V. Q. Dang, R. V. Sabariego, L. Kahenbuhl, and C. Geuzaine, "Correction of Thin Shell Finite Element Magnetic Models via a Subproblem Method," *IEEE Transactions on Magnetics*, vol. 47, no. 5, pp. 1158–1161, May 2011, doi: 10.1109/TMAG.2010.2076794.

[6] V. Q. Dang, P. Dular, R. V. Sabariego, L. Krahenbuhl, and C. Geuzaine, "Subproblem Approach for Thin Shell Dual Finite Element

Formulations," *IEEE Transactions on Magnetics*, vol. 48, no. 2, pp. 407–410, Feb. 2012, doi: 10.1109/TMAG.2011.2176925.

[7] D. Q. Vuong, "Modeling of magnetic fields and eddy current losses in electromagnetic screens by a subproblem method," *TNU Journal of Science and Technology*, vol. 194, no. 1, pp. 7–12, 2019.

[8] V. D. Quoc and C. Geuzaine, "Using edge elements for modeling of 3-D magnetodynamic problem via a subproblem method," *Science and Technology Development Journal*, vol. 23, pp. 439–445, Feb. 2020, doi: 10.32508/stdj.v23i1.1718.

[9] D. Q. Vuong and N. D. Quang, "Coupling of Local and Global Quantities by A Subproblem Finite Element Method – Application to Thin Region Models," *Advances in Science, Technology and Engineering Systems Journal (ASTESJ)*, vol. 4, no. 2, pp. 40–44, 2019, doi: 10.25046/aj040206.

[10] P. Dular, R. V. Sabariego, M. V. Ferreira da Luz, P. Kuo-Peng, and L. Krahenbuhl, "Perturbation Finite Element Method for Magnetic Model Refinement of Air Gaps and Leakage Fluxes," *IEEE Transactions on Magnetics*, vol. 45, no. 3, pp. 1400–1403, Mar. 2009, doi: 10.1109/TMAG.2009.2012643.

[11] V. D. Quoc, "Robust Correction Procedure for Accurate Thin Shell Models via a Perturbation Technique," *Engineering, Technology & Applied Science Research*, vol. 10, no. 3, pp. 5832–5836, Jun. 2020.

[12] S. Koroglu, P. Sergeant, R. V. Sabariego, V. Q. Dang, and M. D. Wulf, "Influence of contact resistance on shielding efficiency of shielding gutters for high-voltage cables," *IET Electric Power Applications*, vol. 5, no. 9, pp. 715–720, Nov. 2011, doi: 10.1049/iet-epa.2011.0081.

[13] K. Abubakri and H. Veladi, "Investigation of the Behavior of Steel Shear Walls Using Finite Elements Analysis," *Engineering, Technology & Applied Science Research*, vol. 6, no. 5, pp. 1155–1157, Oct. 2016.

[14] G. Meunier, *The Finite Element Method for Electromagnetic Modeling*. New York, NY, USA: John Wiley & Sons, Ltd, 2010.

[15] C. Geuzaine, B. Meys, F. Henrotte, P. Dular, and W. Legros, "A Galerkin projection method for mixed finite elements," *IEEE Transactions on Magnetics*, vol. 35, no. 3, pp. 1438–1441, May 1999, doi: 10.1109/20.767236.

[16] P. E. Farrell and J. R. Maddison, "Conservative interpolation between volume meshes by local Galerkin projection," *Computer Methods in Applied Mechanics and Engineering*, vol. 200, no. 1, pp. 89–100, Jan. 2011, doi: 10.1016/j.cma.2010.07.015.

[17] G. Parent, P. Dular, F. Piriou, and A. Abakar, "Accurate Projection Method of Source Quantities in Coupled Finite-Element Problems," *IEEE Transactions on Magnetics*, vol. 45, no. 3, pp. 1132–1135, Mar. 2009, doi: 10.1109/TMAG.2009.2012652.

AUTHOR'S PROFILE

Vuong Dang Quoc received his PhD degree in 2013 from the Faculty of Applied Sciences at the University of Liege in Belgium. After that he came back to the Hanoi University of Science and Technology in September 2013, where he is currently working as the director of the Training Center of Electrical Engineering, School of Electrical Engineering, Hanoi University of Science and Technology. Dr. Vuong Dang Quoc's research domain encompasses modeling of electromagnetic systems by coupling of subproblem method with application to thin shell models.